ARMY RESEARCH LABORATORY

In Silico Methods Shed New Insights Into Cyanide-Caused Cardiac Toxicity

by Csaba K. Zoltani, Steven I. Baskin, and COL G. E. Platoff

ARL-TR-3485 **May 2005**

NOTICES

Disclaimers

The findings in this report are not to be construed as an official Department of the Army position unless so designated by other authorized documents.

Citation of manufacturer's or trade names does not constitute an official endorsement or approval of the use thereof.

Destroy this report when it is no longer needed. Do not return it to the originator.

Army Research Laboratory
Aberdeen Proving Ground, MD 21005-5067

ARL-TR-3485 **May 2005**

In Silico Methods Shed New Insights Into Cyanide-Caused Cardiac Toxicity

Csaba K. Zoltani
Computational and Information Sciences Directorate, ARL

Steven I. Baskin and COL G. E. Platoff
U.S. Army Medical Research Institute of Chemical Defense

Report Documentation Page

Form Approved
OMB No. 0704-0188

1. REPORT DATE *(DD-MM-YYYY)*	2. REPORT TYPE	3. DATES COVERED (From - To)
May 2005	Final	January 2003–August 2003

4. TITLE AND SUBTITLE
In Silico Methods Shed New Insights Into Cyanide-Caused Cardiac Toxicity

5a. CONTRACT NUMBER

5b. GRANT NUMBER

5c. PROGRAM ELEMENT NUMBER

6. AUTHOR(S)
Csaba K. Zoltani, Steven I. Baskin,* and COL G. E. Platoff*

5d. PROJECT NUMBER
3UH7XL

5e. TASK NUMBER

5f. WORK UNIT NUMBER

7. PERFORMING ORGANIZATION NAME(S) AND ADDRESS(ES)
U.S. Army Research Laboratory
ATTN: AMSRD-ARL-CI-HC
Aberdeen Proving Ground, MD 21005-5067

8. PERFORMING ORGANIZATION REPORT NUMBER
ARL-TR-3485

9. SPONSORING/MONITORING AGENCY NAME(S) AND ADDRESS(ES)

10. SPONSOR/MONITOR'S ACRONYM(S)

11. SPONSOR/MONITOR'S REPORT NUMBER(S)

12. DISTRIBUTION/AVAILABILITY STATEMENT
Approved for public release; distribution is unlimited.

13. SUPPLEMENTARY NOTES
*U.S. Army Medical Research Institute of Chemical Defense, Pharmacology Division, Aberdeen Proving Ground, MD 21010-5400

14. ABSTRACT

A high performance computational study of cyanide's (CN's) effect on cardiac tissue is presented. CN's interference with atrial tissue energy production was simulated by studying the effect of the changes in magnitude of the K_{ATP} membrane current on the action potential, thereby understanding the processes leading to the disappearance of the P-wave in the CN-affected tissue. CN was found to render the membrane current levels insufficient to maintain the required wave shape and duration. These results suggest that pharmacological intervention could seek the restoration of ion concentration levels as a possible approach to restoring homeostasis.

15. SUBJECT TERMS
cyanide, cardiac toxicity, high performance computer simulation

16. SECURITY CLASSIFICATION OF:			17. LIMITATION OF ABSTRACT	18. NUMBER OF PAGES	19a. NAME OF RESPONSIBLE PERSON
a. REPORT	b. ABSTRACT	c. THIS PAGE			Csaba K. Zoltani
UNCLASSIFIED	UNCLASSIFIED	UNCLASSIFIED	UL	26	19b. TELEPHONE NUMBER (*Include area code*) 410-278-6650

Standard Form 298 (Rev. 8/98)
Prescribed by ANSI Std. Z39.18

Contents

List of Figures iv

List of Tables iv

Acknowledgments v

1. Introduction 1

2. Cardiac Cell Energy Metabolism 2

3. Metabolic Networks: Work in Progress 3

4. CN-Caused Changes in the ECG of an Adult Male 4

5. An *In Silico* Exploration of CN-Affected Cardiac Tissue 4

6. Results and Discussion 8

7. References 13

Distribution List 16

List of Figures

Figure 1. Significant CN-induced changes in the ECG of an adult male. 5

Figure 2. Effect of CN on the cardiac myocyte. For clarity, not all dependencies and interactions are shown.....6

Figure 3. Effect of ATP concentration changes on the atrial action potential. The top curve denotes the homeostatic condition. The middle curve gives the condition for [ATP] = 2.0 mmol/L, and the bottom curve gives the condition for [ATP] = 1.0 mmol/L. 9

Figure 4. Atrial action potentials under ischemia-like conditions, caused by CN toxicity, that increase the $[Na^+]_i$ and $[K^+]_o$ levels in the tissue. The homeostatic condition (top) is compared with conditions of [ATP] = 1.5 mmol/L (middle) and 1.0 mmol/L (bottom) at $[Na^+]_i$ and $[K^+]_o$ of 17.0 and 12.0 mmol/L, respectively, with a slightly elevated $[Mg^{2+}]$ of 3.5 mmol/L.....10

Figure 5. Contrast of a normal atrial action potential (top) with one when [ATP] is depleted to 2.0 mmol/L and both $[K^+]_o$ and $[Na^+]_i$ are at a subnormal level of 4.5 mmol/L each (bottom).....10

Figure 6. Atrial tissue with $[K^+]_o$ elevated to 12.0 mmol/L ([top] initial resting voltage is no longer reached) and $[Na^+]_i$ elevated to 17.0 mmol/L ([bottom] the resting voltage is depressed, but the trace remains above the original value). 11

Figure 7. Run time as a function of number of processing nodes on the SP-4. 12

List of Tables

Table 1. Summary of significant deviations from the norm found in the ECG of a CN-intoxicated subject. 6

Acknowledgments

The authors thank Dr. John Pormann, Duke University, Durham, NC, for giving expert advice concerning the simulations. This work has also benefited from computer time made available through the Department of Defense High Performance Computing Modernization Program. Computer calculations were done on the IBM SP3 and SP4 at the Major Shared Resource Center, U.S. Army Research Laboratory, Aberdeen Proving Ground, MD.

INTENTIONALLY LEFT BLANK.

1. Introduction

The primary effect of cyanide (CN) on cardiac tissue is its interference with the cellular energy balance, that is, its inhibition of cytochrome oxidase, a mitochondrial enzyme, preventing the transfer of electrons from cytochrome c to molecular oxygen. The impacted aerobic metabolism results in lactic acid acidosis and reduced adenosine triphosphate (ATP) concentration, which lead to anoxia. With a reduction in cellular energy, the following effects develop in tandem: changes in calcium ion concentration in several cellular compartments, calcium current modulation, and inotropic effects (Way, 1984). Simultaneously, a gradual decrease in action potential duration is also noted. The subsidiary cellular processes are still being elucidated, but the sine qua non for developing effective therapeutic regimes is management of these effects. An *in silico* approach that shows how available data and models can be used to develop new therapies is presented in this report.

Toward these ends, an electrocardiogram (ECG) of an individual under CN intoxication is taken as the starting point (Wexler et al., 1947). The deviation from homeostasis, that is, from normal conditions, is interpreted in terms of the modulation of the membrane ionic currents that compose the action potential. The nature of the deviation suggests the pharmacological intervention required to stop and possibly reverse the toxicology.

The need for a therapy to counteract CN poisoning is especially urgent in situations where a dosage of one LD_{50} of CN is encountered, that is, where the dosage of the toxin is ≥0.2 mg/kg of body weight. In these cases, as shown by Ansell and Lewis (1970), Baskin et al. (1987), and Baskin (1991), the poison primarily affects the heart, expressed through its effect on the ventricles. Reminiscent of severe ischemia, lesions in the heart tissue were noted by Suzuki (1968). Upon exposure to the poison, the heart initially slows down into the bradycardia regime, then in time transits to arrhythmia. The ventricles are severely affected, expressed by symptoms of repolarization disorders culminating in Torsade de Pointes (TdP) and ventricular fibrillation (VF).

An overview of cardiac cell energy metabolism is addressed in section 2, setting the stage for a quantification of the changes brought about by CN perturbation of cardiac tissue metabolism. Section 3 delves into the issue of metabolic networks and sketches the opportunities, in conjunction with high performance computing requirements, to deepen our understanding of the cellular processes. This is followed by an interpretation in section 4 of the salient changes in the ECG of a subject under severe CN intoxication. Section 5 shows how *in silico* techniques can shed light on the action potential modulations caused by CN and point to the required characteristics of an antidote. Finally, this report concludes with a discussion of the results in section 6.

2. Cardiac Cell Energy Metabolism

The cardiac myocyte derives its energy primarily from fatty acids, which make up to 90% of the total energy required. The energy is derived from glucose and lactate metabolism (Opie, 1998). The mitochondrion is the source of the ATP produced from adenosine diphosphate (ADP) and inorganic phosphate. Glucose oxidation, though only a minor part of the total energy budget of the cell, plays a crucial role in ion homeostasis. An elaborate system of enzymes regulates the glycolytic pathway. Glycolysis converts glucose to pyruvate, which in turn transforms to acetyl-CoA and enters the Krebs cycle. In a diseased state, the breakdown of glucose or glycogen to lactate replaces the oxidative metabolism for anaerobic energy production. In anoxia, ATP levels decrease with the cessation of oxidative metabolism, and glycolysis provides limited amounts of energy.

The three stages of energy metabolism are (1) Krebs cycle input, (2) Krebs cycle production of nicotinamide adenine dinucleotide (NADH), and (3) oxidative phosphorylation (OxPhos). Oxidization takes place by the electron transport chain, passing electrons to molecular oxygen by means of cytochrome oxidase to form water.

The Krebs cycle and glycolysis act as depositories for the energy obtained from substrate catabolism. The Krebs cycle products are oxidized by the electron transport chain. ATP production is controlled at the substrate level by F_1F_0-ATPase and by ADP through a negative feedback mechanism. That is, an increase in ATP/ADP ratio inhibits OxPhos. Also, homeostasis requires control of magnesium and calcium ion levels (Wang et al., 2003).

Energy metabolism is subject to a number of pathologies. Oxygen uptake reduction caused by CN intoxication leads to a slowing of OxPhos and an increase in NADH levels. Also, cell acidification, increased ADP and creatine production, and decreased creatine phosphate production are observed. Mitochondrial myopathies and cytosolic pathologies have been studied, shedding light on respiratory chain defects in electron transport and substrate defects in fatty acid utilization. Cytochrome oxidase deficiency, respiratory chain defects, and decreases in enzyme activity affect the cellular energy metabolism.[*]

Calcium balance controls mitochondrial respiration. Mitochondrial calcium acts like a buffer for the cytosol. Its importance is underlined by the fact that excess calcium under cytosolic calcium overload conditions limits the proton gradient, thereby limiting the synthesis of ATP.

This short summary of energy metabolism has not touched upon many of the subsidiary issues, including the kinetics of key regulatory enzymes, substrates, and products (Balaban, 2002; Jafri et al., 2001). Rather, our aim is to apprise the reader of the need to consider the transformations

[*] Letellier et al. (1994, 1998) have modeled the block of cytochrome oxidase by cyanide using metabolic control analysis.

and components of metabolic networks when trying to understand the processes accompanying CN intoxication. Respiration interference is not the only process that may play a determining role.

3. Metabolic Networks: Work in Progress

Metabolic and protein networks of toxin-intoxicated tissues contain a wealth of information needed for the development of antidotes and therapies. The networks are best pictured as nodes and links. The node may be a substrate or a protein, and the link is the interaction between two chemical nodes—a chemical transformation. The interconnected nodes form a structure.

The last few years have witnessed an explosion in the understanding of live and inanimate network structures and the attempts to relate them to performance. The research of Barabasi and his group (Albert and Barabasi, 2001; Barabasi, 2002; Jeong et al., 2000) showed that a network's topology is the key to its dynamic behavior and robustness when under attack. A notable insight gained from tests on 43 organisms is that their structures are scale-free, that is, no single node represents all of the nodes. In fact, the node distribution follows a power law—a few nodes are linked with many neighbors, forming hubs, but the vast majority have only a few neighbors. The hubs also lend heterogeneity to the topology. To test the robustness of the system to perturbations, links are removed at random. Most deletions do not affect the overall system function, but hub removal does. In a biological network as well as the internet, hub removal is catastrophic in the sense that the network is no longer able to function as intended. For example, catalytic enzymes may be removed from an organism without adverse effect on its overall performance, but if any of the hubs are removed, the consequences could be disastrous.

Questions about the effect threat agents have on an organism can be reformulated in terms of networks. Identifying the affected link gives clues about the cellular problem and possibly points to alternative or compensatory links that could be established to overcome the network fault, a fault that may adversely affect the organism's ability to function.

Further means to understanding the mechanisms involved in the action of toxins include the study of metabolic network topology, the identification of hubs, and the study of the kinetics that regulate the links coupled with flux analysis (Bhalla and Iyengar, 1999). They shed light on the need for the survival of certain node-link combinations and, if injured, the alternate routes or actions that would enhance the likelihood of their survival. Along these lines, ancillary work has been performed to determine the effect of deleting (or turning off) certain genes on red blood cell function and *Escherichia coli*. For the cardiac myocyte network, ATP is a hub. Its deletion or isolation leads to apoptosis, cell death. This is explored further in section 5.

4. CN-Caused Changes in the ECG of an Adult Male

A Lead I ECG from a NaCN-gas-intoxicated adult male, at a lethal dose level of 0.2 mg/kg of body weight, is shown in figure 1. The ECG traces, interpreted in terms of myocyte membrane currents, give a time-resolved record of CN's effect on the heart. Some of the significant anomalies and deviations from the norm in this ECG include the following:

1. The initial heart rate (HR) is 150 beats/min (BM), which changes to a rate of 37.5 BM at time t = 3 min, signaling bradycardia. At t = 5 min, the rate increases to 54.5 BM, and at t = 10 min, before severe arrhythmia develops, it increases to 85.7 BM.
2. Morphological changes in the T-wave (the repolarization of the ventricles) are apparent from t = 3 min on. There is a notable widening of the base of the wave and a fusing of the T-wave with the QRS-complex.
3. The ST-segment represents the early part of the ventricular repolarization. Under normal conditions, its duration is ≤0.2 s depending on the HR. An ST-segment changed by more than 1.0 mm from the horizontal, homeostatic position signals widespread myocardial injury, usually of the transmural kind (Li et al., 2000; Yan and Antzelevitch, 1999). Such a change is evident in figure 1.
4. The P-wave is missing. By t = 3 min, the P-wave has disappeared, indicating no atrial activity. Absence of the P-wave persists from that time on.

Table 1 summarizes some of the deviations from the norm found in the CN-intoxicated individual's ECG and relates them to the myocyte membrane currents.

5. An *In Silico* Exploration of CN-Affected Cardiac Tissue

The ECG modulation caused by changes in the myocyte's membrane current is used as the basis for probing CN's effect on cell electrophysiology. Effects that diminish or block membrane currents dictate the requirements for the therapeutic agent. Computer simulations identify the cellular parameters that are most effective in controlling these changes.

Available models (figure 2) consider only indirectly, if at all, the effect of metabolic changes, especially those caused by disease, on cell electrophysiology. Myocardial ischemia causes anoxia, acidosis, and an increase in potassium concentration. In some respects, it is characterized by symptoms analogous to CN intoxication. A number of ischemia models have been proposed (Ferrero et al., 1996; Shaw and Rudy, 1997) and snapshots have been given of the action potentials calculated for specific levels of ATP, based on experimental observations

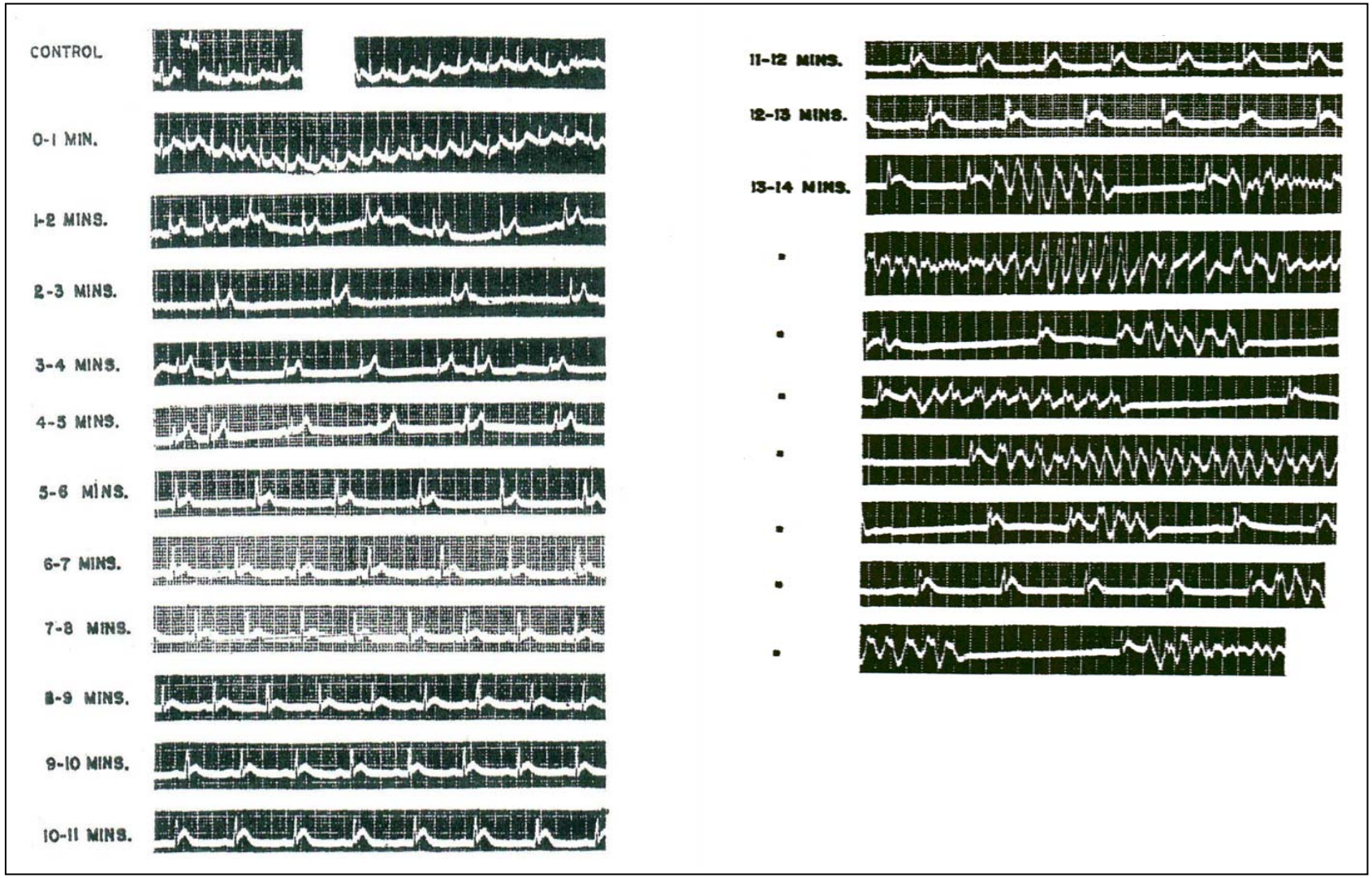

Figure 1. Significant CN-induced changes in the ECG of an adult male.*

*Reprinted from the *American Heart Journal* (Wexler et al., 1947) with permission from Elsevier Science: New York. Additional discussion of ECG modulation due to CN is given in Katzman and Penney (1993) and Salkowsky and Penney (1995).

Table 1. Summary of significant deviations from the norm found in the ECG of a CN-intoxicated subject.

Symptom	Possible Cause	Primary Membrane Current (I) Affected
P-wave disappearance	Auricular arrest	Depolarization of left and right atria by I_{Na}
T-wave modulation Peaked upright Inverted Polarity, width	 Subendocardial ischemia Subepicardial ischemia Gap junction resistance	Abnormal repolarization, I_K
ST-segment elevation, shortening, and disappearance	Ischemia, hyperkalemia	I_{KATP} activation, I_{Na} inactivation, Brugada syndrome
QRS-complex right-axis deviation	Right bundle branch/left posterior vascular block	Depolarization currents of right and left ventricles
Wenckebach phenomenon (progressive lengthening of PR-interval until absence of QRS-complex)	Defective conduction through atrioventricular (AV) node	—
Bradycardia (HR < 50 BM)	AV block, prolonged conduction between atria and ventricles	Decreased $I_{Ca(L)}$ activity
Tachycardia (HR > 100 BM)	Increased activity of adrenergic system	I_f in sinus node
TdP, VF	Various, including QT-interval lengthening	—

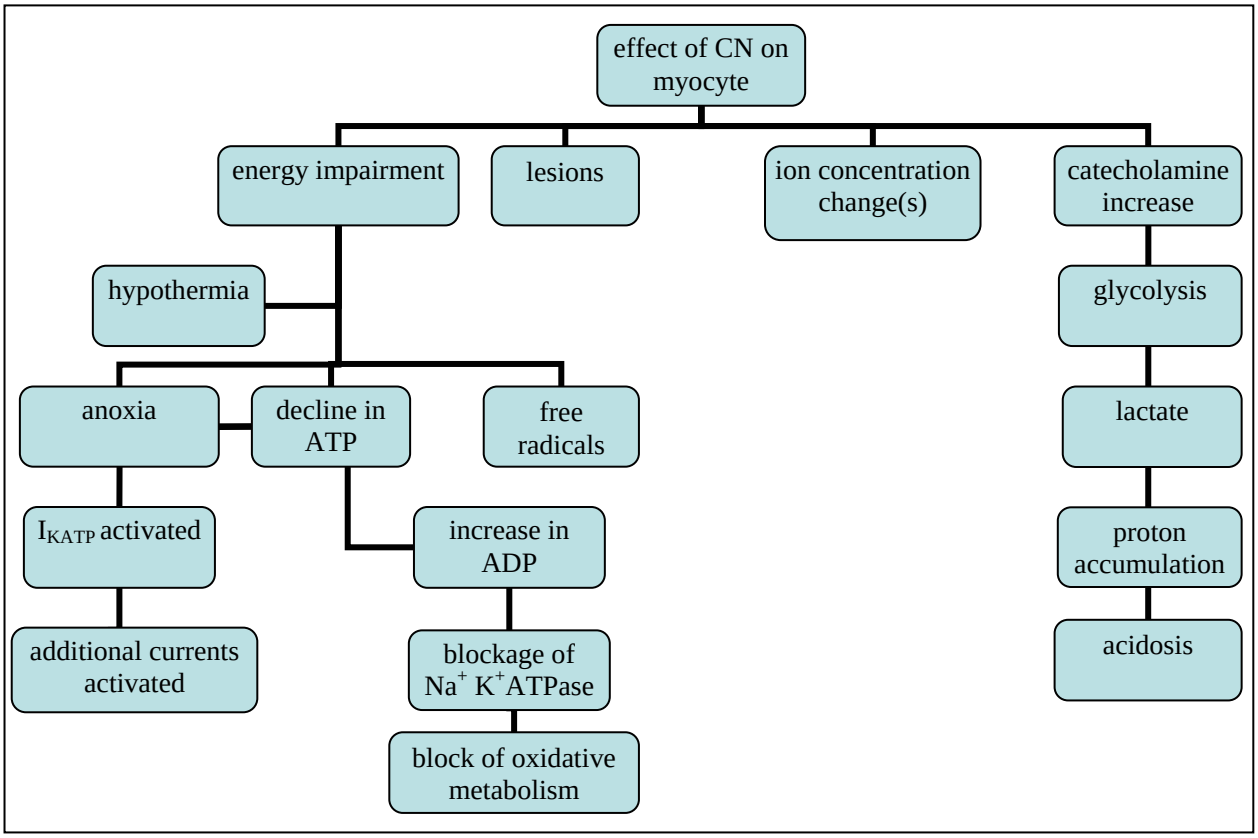

Figure 2. Effect of CN on the cardiac myocyte. For clarity, not all dependencies and interactions are shown.

that, in anoxia, the ancillary metabolic changes lead to a decline in ATP concentration. Below an ATP concentration threshold, the I_{KATP} is activated, which in turn affects the action potential duration and shape (Elliott et al., 1989; Light et al., 2001; Nichols et al., 1991). These concepts can be extended to explain the ECG changes from CN intoxication.

CN inhibits cytochrome c oxidase activity, which in turn causes a decrease in the mitochondrial respiration and exhibits a threshold behavior akin to some of the mitochondrial diseases. The decline in ATP concentration opens K_{ATP} channels (Borowitz et al., 2001). Also, increases in catecholamine levels, thought to contribute to the genesis of arrhythmias (Baskin et al., 1987), intracellular sodium accumulation (Kupriyanov et al., 1996), increases in inorganic phosphate, lactate production, and elevated calcium levels (Kondo et al., 1998), are noted. This report addresses the issue of ATP concentration change effects on the I_{KATP} in atrial tissue.

Atrial K_{ATP} currents are not completely understood at the present time. Baron et al. (2001) reported that pituitary adenylate cyclase-activating polypeptide (PACAP) activates the I_{KATP} in rat atrial myocytes through the protein kinase A and protein kinase C pathways. PACAP at 1 nmol/L activates a current of 85 pA/pF compared to 26 pA/pF with 5 mmol/L of ATP. A number of peptides present in the heart, including vasoactive intestinal peptide, also activate the I_{KATP}, though not as effectively as PACAP. Thus, the ultimate model will have to take several subsidiary, and heretofore neglected, events into account.

Metabolic impairment that activates the I_{KATP} is thought to have cardioprotective function in ischemia but also shortens the action potential duration explained on the basis of increased $[K^+]_o$. Several models of the I_{KATP} exist. Ferrero et al. (1996) and Shaw and Rudy (1997) have included it in their models of ventricle electrophysiology. These models propose a relationship between the current density and ATP concentration and give snapshots of the tissue state as the I_{KATP} is activated. Since CN intoxication shares a number of characteristics with ischemia, including anoxia and acidosis, models of the latter are convenient starting points for CN-affected tissue simulation. The effect of the CN loading on the atrial tissue is modeled by expressing the I_{KATP} and adjusting the potassium and sodium concentrations and the $I_{Ca(L)}$.

A modified atrial model (Nygren et al., 1998) is used to demonstrate that modulation of the potassium currents, especially when the I_{KATP} is present, can explain the AV blockage that is expressed by the P-wave disappearing from the ECG during CN poisoning. For this purpose, an ATP-dependent current is added to the membrane model and expressed as follows:

$$I_{KATP} = \text{fac1} * \text{fac2} * \text{fac3} * f_{ATP} * (V_m - E_K), \quad (1)$$

where fac1 is the channel density (~4.0 channels/μm^2), fac2 is the channel conductance (~40.0×10^{-3} nS/cm^2), fac3 is the effect of the presence of magnesium ions, f_{ATP} is a function of the ATP concentration, V_m is the voltage in the membrane, and E_K is the Nernst potential.

In the resting state, the ATP concentration is taken as 5 mmol/L. Three cases are calculated: (1) when the membrane is at rest, (2) when the ATP concentration is reduced by 50%, and (3) when all of the ATP has been used.

For the calculations reported, the monodomain model of cardiac tissue is assumed to be valid. The properties of the cells are averaged over the whole domain without taking the anisotropy of the cardiac tissue into account. The action potential propagation is determined by solving the following equation:

$$\frac{\partial v}{\partial t}(\bar{x},t) = \frac{1}{C_m}\left[-i_{ion}(\bar{x},t) - i_{stim}(\bar{x},t) + \frac{1}{\beta}\left(\frac{\kappa}{\kappa+1}\right)\nabla \circ (D_i(\bar{x})\nabla v(\bar{x},t)) \right], \qquad (2)$$

where v is the voltage, i is the current, and β and κ characterize the tissue with D_i as the diffusion coefficient.

Obtaining a typical solution (i.e., the time-resolved electrophysiological state of the atria) for 300-ms real time in a tissue of 3 × 3 cm required 7 hr of nondedicated time using 16 processors. Data was stored at 5-ms intervals, and TIFF files were constructed using voltages as functions of position in the two-dimensional plane of the tissue. The panels displayed were constructed using Tecplot, version 9.01.

6. Results and Discussion

CN's interference with atrial tissue energy production was simulated by studying the effect of the changes in magnitude of the I_{KATP} on the action potential, thereby understanding the processes leading to the disappearance of the P-wave in the CN-affected tissue. Also, ischemic conditions were used as the hypothesized state of the tissue with the $I_{Ca(L)}$ partially blocked.

Figure 3 shows the atrial action potential at several concentrations of ATP, starting with the normal, homeostatic and corresponding to [ATP] at >6.0, at 2.0, and at 1.0 mmol/L, respectively. Notable shortening of the action potential is observed from 300 ms down to 10 ms at [ATP] = 1.0 mmol/L. In tandem, the slope of the repolarization changes. The maximum value of the membrane voltage drops from ~20 mV to the single-digit values under conditions of increased $[Na^+]_i$ and $[K^+]_o$, that is, accumulated sodium ions inside of the cell and potassium ions outside of the cell. When the potassium and sodium are held at homeostatic values, the action potential does not reach the threshold voltage, indicating impending shutdown of the cell.

Drastic shortening of the action potential cycle is observed under conditions of elevated potassium and sodium concentrations (figure 4), with a slightly elevated magnesium concentration at 3.5 mmol/L (approximating CN-toxicity conditions) and a 75% block of the $I_{Ca(L)}$.

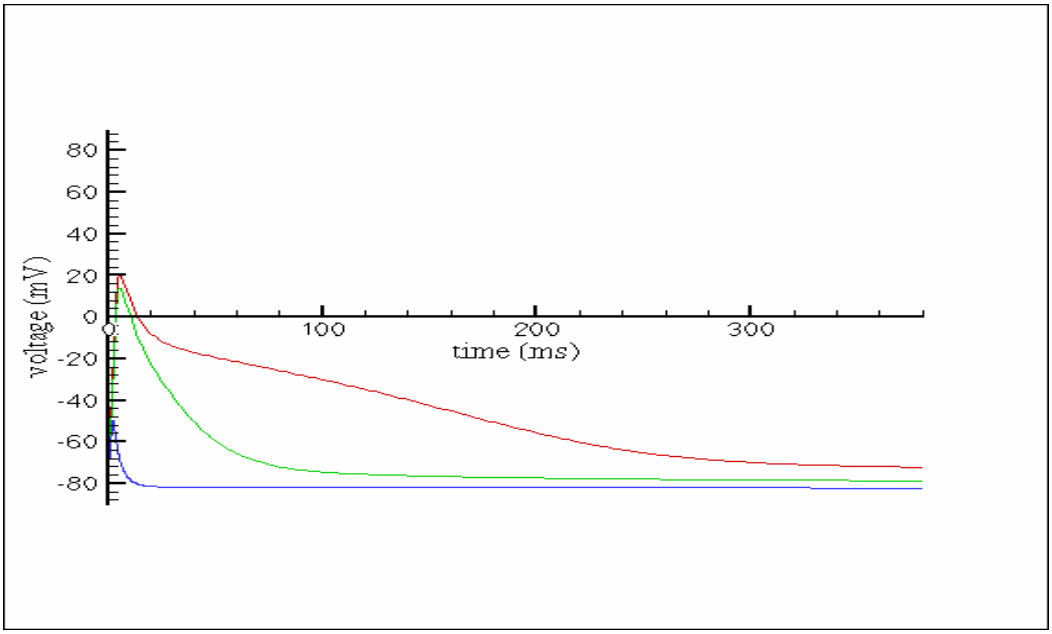

Figure 3. Effect of ATP concentration changes on the atrial action potential. The top curve denotes the homeostatic condition. The middle curve gives the condition for [ATP] = 2.0 mmol/L, and the bottom curve gives the condition for [ATP] = 1.0 mmol/L.

Again, the homeostatic cycle length (CL) of ~300 ms is shortened to 10 ms at [ATP] = 2.0 mmol/L, with CL = <10 ms at [ATP] = 1.0 mmol/L. The action potential maximum voltage value stays positive though considerably lower, ~8.0 mV, than the normal value. Also, the voltage never returns to the baseline value of –74.0 mV but approaches –68.0 mV.

At elevated $[Na^+]_i$ values of 17.0 mmol/L, the action potential hyperpolarizes. The hyperpolarization disappears as the $[K^+]_o$ is elevated. Under these conditions, the normal resting voltage is never reached.

Figure 5 contrasts the normal action potential with the case when [ATP] = 2.0 mmol/L and $[Na^+]_i$ = 4.5 mmol/L, a subnormal condition when $[K^+]_o$ is held at 4.5 mmol/L. Again, the CL is shortened, the maximum amplitude is lowered, and the slope of the repolarization changes drastically.

The reduction in time available for the depolarization to take place (figure 6) as well as the voltage amplitude observed under these conditions makes a strong case for the diminution and eventual complete disappearance of the P-wave from the ECG. Also, blockage of the depolarization wave is a plausible scenario.

The study described in this report addresses only indirectly the effects of calcium ion flow and concentration changes by including a partial block of the $I_{Ca(L)}$. The rundown of the ATP energy supply for the sarcoplasmic reticulum pump that transfers calcium ions into the extracellular

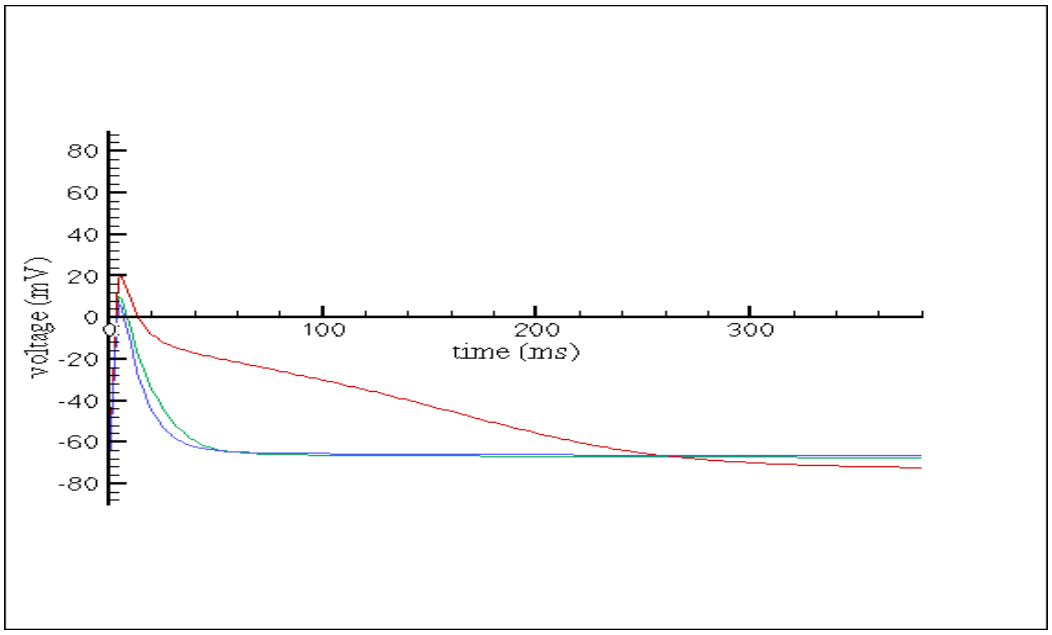

Figure 4. Atrial action potentials under ischemia-like conditions, caused by CN toxicity, that increase the $[Na^+]_i$ and $[K^+]_o$ levels in the tissue. The homeostatic condition (top) is compared with conditions of [ATP] = 1.5 mmol/L (middle) and 1.0 mmol/L (bottom) at $[Na^+]_i$ and $[K^+]_o$ of 17.0 and 12.0 mmol/L, respectively, with a slightly elevated $[Mg^{2+}]$ of 3.5 mmol/L.

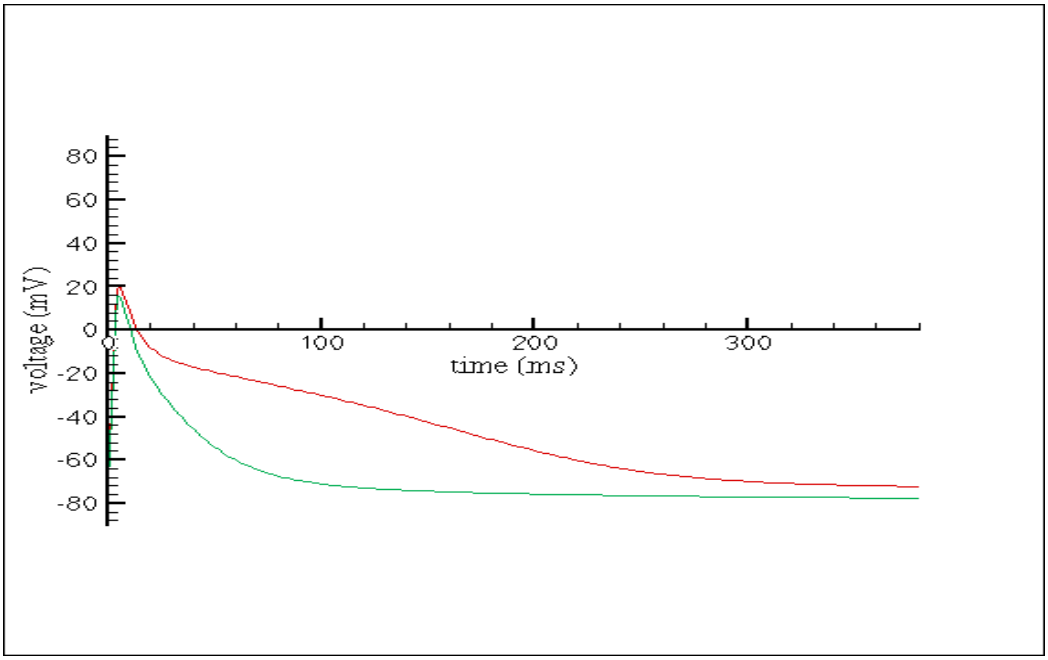

Figure 5. Contrast of a normal atrial action potential (top) with one when [ATP] is depleted to 2.0 mmol/L and both $[K^+]_o$ and $[Na^+]_i$ are at a subnormal level of 4.5 mmol/L each (bottom).

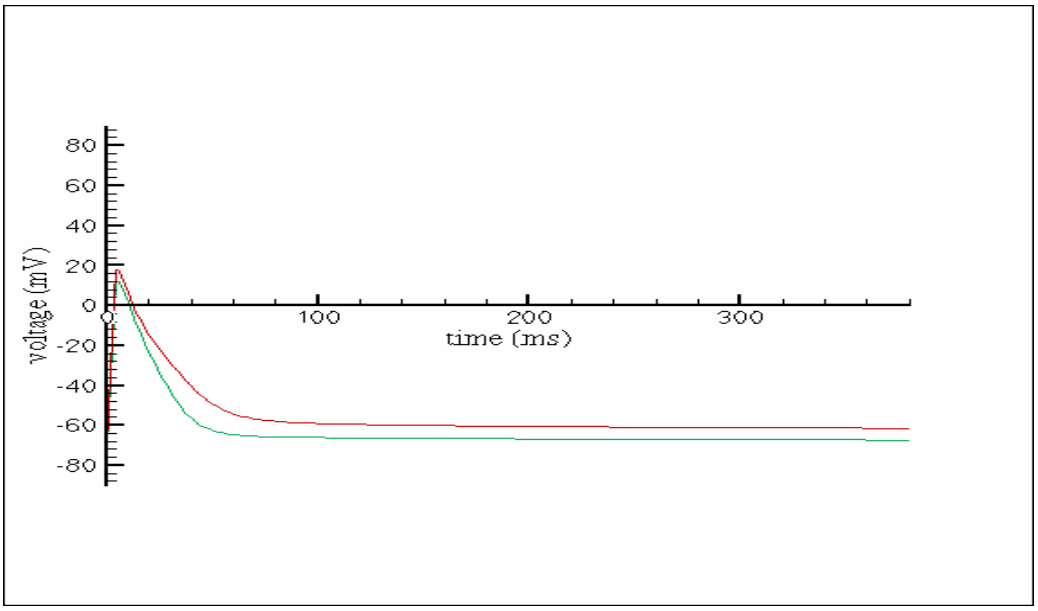

Figure 6. Atrial tissue with $[K^+]_o$ elevated to 12.0 mmol/L ([top] initial resting voltage is no longer reached) and $[Na^+]_i$ elevated to 17.0 mmol/L ([bottom] the resting voltage is depressed, but the trace remains above the original value).

space against a concentration gradient leads to calcium overload. This may lead to abnormal calcium-induced currents, which are precursors to arrhythmia. Changes in action potential morphology express, and possibly contribute to, the modulation of the $I_{Ca(L)}$. The threshold for the activation of this current in myocytes is around –25 mV. Half-maximum deactivation is observed at or below –20 mV. One of CN's effects on action potentials is the narrowing of the area under the curve with the decline in ATP availability. This is signaled by an increase in the angle, measured from the horizontal, from the maximum of the voltage-vs.-time plots. The narrowing indicates a decrease in the time that the calcium ion channels remain open and operative and, thus, the amount of calcium ions that are transferred. Consequently, the total ion flow is reduced.

The electrophysiological changes caused by CN intoxication of the atria lead to profound changes in the membrane currents needed to maintain the P-wave in an ECG. Indeed, the effect of the CN is to render the membrane current levels insufficient for maintaining the required wave shape and duration. These results suggest that pharmacological intervention could seek the restoration of ion concentration levels as a possible approach to restoring homeostasis.

The simulation of cardiac toxicity with ancillary markers generated by the pathology requires consideration of a tissue domain large enough to allow the cellular processes to establish a basis that leads to wave propagation and other manifestations of the modulation of the electrophysiologic processes. A myocyte is typically 100 × 20 μm, thus even a small patch of tissue consists of a very large number of cells. A simulation based on cellular processes requires sizeable computational assets.

The computational resources required for the calculation of a 1 × 1 cm piece of tissue is shown in figure. 7. When fewer than 16 processors are used, the computational times become prohibitive, jumping from 1830 s for 16 processors to 3356 s for 8 processors and 6566 s for 4 processors. The scalability of the algorithm is apparent. The processing time with 64 processors was 611 s, underlining the advantage of parallel processing.

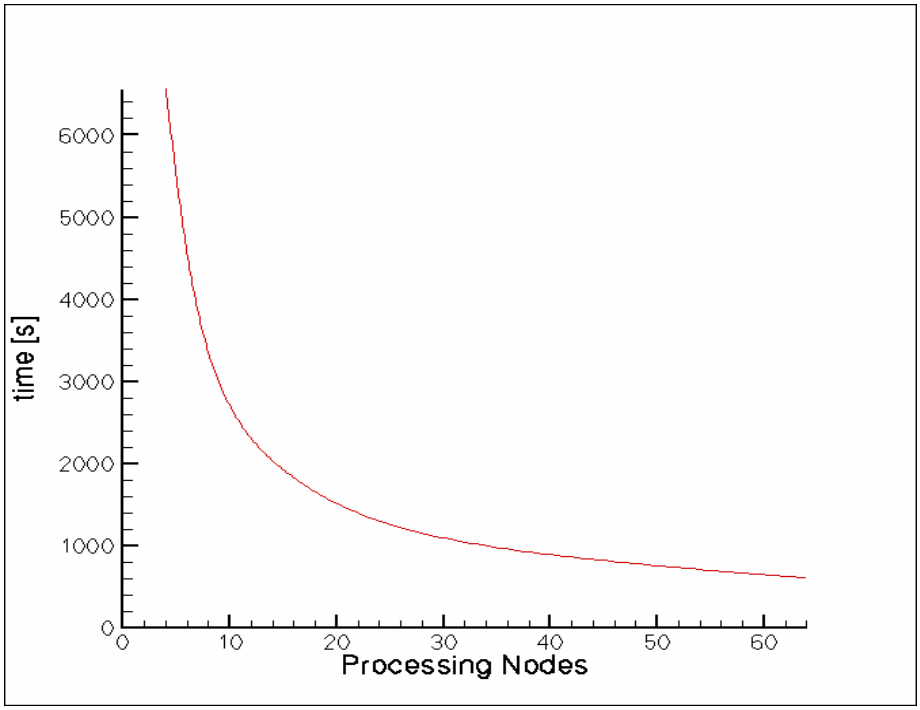

Figure 7. Run time as a function of number of processing nodes on the SP-4.

7. References

Albert, R.; Barabasi, A.-L. Statistical Mechanics of Complex Networks. *Physiol. Rev.* **2001**, *1–54*.

Ansell, M.; Lewis, F. A. S. A Review of Cyanide Concentrations Found in Human Organs. *J. Forensic Med.* **1970**, *17*, 148–154.

Balaban, R. S. Cardiac Energy Metabolism Homeostasis: Role of Cytosolic Calcium. *J. Mol. Cell. Cardiol.* **2002**, *34*, 1259–1271.

Barabasi, A.-L. *Linked: The New Science of Networks*; Perseus Publishing: Cambridge, MA, 2002.

Baron, A.; Monnier, D.; Roatti, A.; Baertschi, A. J. Pituitary Adenylate Cyclase-Activating Polypeptide Activates K_{ATP} Current in Rat Atrial Myocytes. *Am. J. Physiol. Heart Circ. Physiol.* **2001**, *280*, H1058–H1065.

Baskin, S. I., Ed. The Cardiac Effects of Cyanide. In *Cardiac Toxicology*; CRC Press: Boca Raton, FL, 1991; pp 419–430.

Baskin, S. I.; Wilkerson, G.; Alexander, K.; Blitstein, A. G. Cardiac Effects of Cyanide. In *Clinical and Experimental Toxicology of Cyanides*; Ballantyne, B., Marrs, T. C., Eds.; Wright: Bristol, England, 1987; pp 138–155.

Bhalla, U. S.; Iyengar, R. Emergent Properties of Networks of Biological Signaling Pathways. *Science* **1999**, *283*, 381–387.

Borowitz, J. L.; Isom, G. E.; Baskin, S. I. Acute and Chronic Cyanide Toxicity. In *Chemical Warfare Agents: Low Level Toxicity*; Somani, S., Romano, J. A., Jr., Eds.; CRC Press: Boca Raton, FL, 2001; pp 301–319.

Elliott, A. C.; Smith, G. L.; Allen, D. G. Simultaneous Measurements of Action Potential Duration and Intracellular ATP in Isolated Ferret Hearts Exposed to Cyanide. *Circ. Res.* **1989**, *64*, 583–591.

Ferrero, J. M., Jr.; Saiz, J.; Ferrero, J. M.; Thakor, N. V. Simulation of Action Potentials From Metabolically Impaired Cardiac Myocytes. *Circ. Res.* **1996**, *79*, 208–221.

Jafri, M. S.; Dudycha, S. J.; O'Rourke, B. Cardiac Energy Metabolism: Models of Cellular Respiration. *Annu. Rev. Biomed. Eng.* **2001**, *3*, 57–81.

Jeong, H.; Tombor, B.; Albert, R.; Oltvai, Z. N.; Barabasi, A.-L. The Large-Scale Organization of Metabolic Networks. *Nature* **2000**, *407*, 651–654.

Katzman, G. M.; Penney, D. G. Electrocardiographic Responses to Carbon Monoxide and Cyanide in the Conscious Rat. *Toxicol. Lett.* **1993**, *69*, 139–153.

Kondo, R. P.; Apstein, C. S.; Eberli, F. R.; Tillotson, D. L.; Suter, T. M. Increased Calcium Loading and Inotropy Without Greater Cell Death in Hypoxic Rat Cardiomyocytes. *Am. J. Physiol*. **1998**, *275*, H2272–H2282.

Kupriyanov, V. V.; Yang, L.; Deslauriers, R. Cytoplasmic Phosphates in Na^+–K^+ Balance in KCN-Poisoned Rat Heart: A ^{87}Rb-, ^{23}Na-, and ^{31}P-NMR Study. *Am. J. Physiol.* **1996**, *270*, H1303–H1311.

Letellier, T.; Heinrich, R.; Malgat, M.; Mazat, J. P. The Kinetic Basis of Threshold Effects Observed in Mitochondrial Diseases: A Systematic Approach. *Biochem. J.* **1994**, *302*, 171–174.

Letellier, T.; Malgat, M.; Rossignol, R.; Mazat, J. P. Metabolic Control Analysis and Mitochondrial Pathologies. *Mol. Cell. Biochem.* **1998**, *184*, 409–417.

Light, P. E.; Kanji, H. D.; Fox, J. E. M.; French, R. J. Distinct Myoprotective Roles of Cardiac Sarcolemmal and Mitochondrial K_{ATP} Channels During Metabolic Inhibition and Recovery. *FASEB J.* **2001**, *15*, 2586–2594.

Li, R. A.; Leppo, M.; Miki, T.; Seino, S.; Marban, E. Molecular Basis of Electrocardiographic ST-Segment Elevation. *Circ. Res.* **2000**, *87*, 837–839.

Nichols, C. G.; Ripoll, C.; Lederer, W. J. ATP-Sensitive Potassium Channel Modulation of the Guinea Pig Ventricular Action Potential and Contraction. *Circ. Res.* **1991**, *68*, 280–287.

Nygren, A.; Fiset, L.; Firek, J. W.; Clark, D. S.; Lindblad, R. B.; Giles, W. R. Mathematical Model of an Adult Human Atrial Cell. The Role of K^+ Currents in Repolarization. *Circ. Res.* **1998**, *82*, 63–81.

Opie, L. H. *The Heart: Physiology, From Cell to Circulation*; Lippincott Williams & Wilkins: Philadelphia, PA, 1998.

Shaw, R. M.; Rudy, Y. Electrophysiologic Effects of Acute Myocardial Ischemia. *Circ. Res.* **1997**, *80*, 124–138.

Suzuki, T. Ultrastructural Changes of Heart Muscle in Cyanide Poisoning. *Tohoku J. Exp. Med.* **1968**, *95*, 271–287.

Salkowsky, A. A.; Penney, D. G. Metabolic, Cardiovascular, and Neurologic Aspects of Acute Cyanide Poisoning in the Rat. *Toxicol. Lett.* **1995**, *75*, 19–27.

Wang, Y. X.; Zheng, Y. M.; Abdullaev, I.; Kotlikoff, M. I. Metabolic Inhibition With Cyanide Induces Calcium Release in Pulmonary Artery Myocytes and *Xenopus* Oocytes. *Am. J. Physiol. Cell. Physiol.* **2003**, *284*, C378–C388.

Way, J. L. Cyanide Intoxication and Its Mechanism of Antagonism. *Annu. Rev. Pharmacol. Toxicol.* **1984**, *24*, 451–481.

Wexler, J.; Whittenberger, J. L.; Dumke, P. R. The Effect of Cyanide on the Electrocardiogram of Man. *Am. Heart J.* **1947**, *34*, 163–173.

Yan, G. X.; Antzelevitch, C. Cellular Basis for the Brugada Syndrome and Other Mechanisms of Arrhythmogenesis Associated With ST-Segment Elevation. *Circulation* **1999**, *100*, 1660–1666.

NO. OF COPIES ORGANIZATION

1 (PDF ONLY) DEFENSE TECHNICAL INFORMATION CTR
DTIC OCA
8725 JOHN J KINGMAN RD
STE 0944
FORT BELVOIR VA 22060-6218

1 US ARMY RSRCH DEV & ENGRG CMD
SYSTEMS OF SYSTEMS INTEGRATION
AMSRD SS T
6000 6TH ST STE 100
FORT BELVOIR VA 22060-5608

1 INST FOR ADVNCD TCHNLGY
THE UNIV OF TEXAS
AT AUSTIN
3925 W BRAKER LN STE 400
AUSTIN TX 78759-5316

1 US MILITARY ACADEMY
MATH SCI CTR EXCELLENCE
MADN MATH
THAYER HALL
WEST POINT NY 10996-1786

1 DIRECTOR
US ARMY RESEARCH LAB
IMNE ALC IMS
2800 POWDER MILL RD
ADELPHI MD 20783-1197

3 DIRECTOR
US ARMY RESEARCH LAB
AMSRD ARL CI OK TL
2800 POWDER MILL RD
ADELPHI MD 20783-1197

3 DIRECTOR
US ARMY RESEARCH LAB
AMSRD ARL CS IS T
2800 POWDER MILL RD
ADELPHI MD 20783-1197

NO. OF COPIES ORGANIZATION

ABERDEEN PROVING GROUND

1 DIR USARL
AMSRD ARL CI OK TP (BLDG 4600)

NO. OF
COPIES ORGANIZATION

ABERDEEN PROVING GROUND

10 USAMRICD
PHARMACOLOGY DIV
S BASKIN (5 CPS)
G PLATOFF (5 CPS)
APG MD 21010-5400

INTENTIONALLY LEFT BLANK.